Int J Pharm Bio Sci 2013 July; 4(3): (B) 181 - 193

Research Article **Bioinfomatics**

International Journal of Pharma and Bio Sciences **ISSN 0975-6299**

IN SILICO CHARACTERIZATION OF HUMAN TYROSINASE USING COMPUTATIONAL TOOLS AND SERVERS

SEN GUPTA, PARTH SARTHI[1]., MONDAL, BUDDHADEV[2] AND BANDYOPADHYAY AMAL KUMAR[*3]

*[*3], [1] Department of Biotechnology, The University of Burdwan, Golapbag, Burdwan, 713104, West Bengal, India.*
[2] Burdwan Raj College, Burdwan University, Burdwan, 713104, West Bengal, India

ABSTRACT

In this paper, sequences of six human tyrosinase, retrieved from Swiss Prot database are analyzed and characterized using *In silico* tools. Primary structure analysis shows that most of the tyrosinase are hydrophobic in nature due to the high content of non -polar residues. The presence of cysteines in the most of the tyrosinases sequences infer that these proteins may form disulphide (SS) bonds, which are regarded as a positive factor for stability. The aliphatic index computed by Ex-Pasy's ProtParam infers that tyrosinases may be thermolabile for a wide range of temperature. Secondary structure analysis shows that some of the tyrosinases have predominant *α*-helical structures and rest of the tyrosinases have mixed secondary structure. The very high coil structural content of most of the sequences is due to the rich content of more flexible glycine and hydrophobic proline amino acids. Proline has a special property of creating kinks in polypeptide chains and disrupting ordered secondary structure. The number of cleaveges and the site of cleavage of the enzyme chymotrypsin and trypsin is calculated by the Ex-Pasy's peptide cutter tool for all the six sequences of tyrosinase.SOSUI server predicts transmembrane regions in P14679, P40126, P17643, Q04671and P21583 tyrosinases. EMBOSS pepwheel is used for generating helical wheel plot from the predicted transmembrane region.The presence of disulphide (SS) bonds in the tyrosinases P98187, P14679, P40126, P17643, Q04671, 075030 and P21583 are predicted by CYS_REC tool, and the homology model of P14679 is visualized using Rasmol & Swiss-Pdb Viewer (SPDBV) tools. Homology model of P14679 is good as the evaluation parameters are within the acceptable limits for the modeled 3D structures.

KEYWORDS:Tyrosinase; computational analysis; disulphide bridges; homology modeling; proteomics tools.

BANDYOPADHYAY AMAL KUMAR
Asst. Professor, Department of Biotechnology, The University of Burdwan, Golapbag, Burdwan, 713104, West Bengal, India.

**Corresponding author*

1. INTRODUCTION

Computational packages and online servers are the current tools used in the protein sequence analysis and characterization.[1] the physicochemical and the structural properties of the proteins are well under-stood with the use of computational tools. Today, number of computational tools has been developed for making predictions regarding the identification and structure prediction of proteins. The statistics about a protein sequence such as number of amino acid, sequence length, and the physicochemical properties of a proteins such as molecular weight, atomic com-position, extinction coefficient, GRAVY, aliphatic index, instability index, etc. can be computed by computational tools for the prediction and characterization of protein structure. The amino acid sequence provides most of the information required for determining and characterizing the molecule's function, physical and chemical properties. Sequence analysis and physicochemical characterization of proteins using biocomputation tools have been done by many researchers and reported.[2–8] Tyrosinase is a well-known copper-containing enzyme and is widely distributed in microorganisms, plants and animals. In fungi and vertebrates, tyrosinase catalyzes the rate-limiting step in the formation of the pigment melanin from tyrosine. In plants, the physiological substrates contain a variety of phenolics. Tyrosinase oxidizes them in the browning pathway, observed when the plant tissues are injured. The tyrosinase extracted from the champignon mushroom, *Agaricus bisporus,* is highly homologous with the mammalian ones. Hence, mushroom tyrosinase is well suited as a model for studies on melanogenesis. Actually, almost all studies on tyrosinase inhibition conducted so far have used mushroom tyrosinase, because only the enzyme is commercially available. Tyrosinase has been ascribed other functions apart from melanin production, including the detoxification of host plant defensive phenols for symbiotic bacteria the sclerotisation of insect cuticles and the synthesis of amino acid based antibiotics. Recently, the activities of tyrosinase have been used in several biotechnological applications. Tyrosinase has been applied in numerous of electrochemical biosensors, for a lot of phenolic compounds. Also, tyrosinase has been applied to activate the tyrosine residues in polypeptides for protein cross-linking tochitosan films, as well as in direct protein-protein cross-linking. Besides, tyrosinases could be applied to the removal of phenol from wastewater and the bioconversion of L-tyrosine to L-DOPA. A mutation in the tyrosinase gene resulting in impaired tyrosinase production leads to type I oculocutaneous albinism, a hereditary disorder that affects one in every 17,000 people. Tyrosinase activity is very important. If uncontrolled during melanoma, it results in increased melanin synthesis. Several polyphenols including flavonoids or stilbenoid, substrate analogues, free radical scavengers and copper chelators have been known to inhibit tyrosinase. Henceforth, the medical and cosmetic industries are focussing a lot of research on tyrosinase inhibitors to treat skin disorders. Numerous structure and function studies have been reported from time to time from all over the world.[9-20] However, physicochemical characterization of tyrosinase has not been done so far. In this paper, we report the *In silico* analysis and characterization studies on tyrosinases of human.

2. MATERIALS AND METHODS

2.1 tyrosinase sequences

Tyrosinase sequences were retrieved from the manually curated public protein database Swiss-Prot.[21] Swiss-Prot is scanned for the key word tyrosinase and then click on the taxonomy, the search result yielded various taxonomic groups. From this we retrieved 6 reviewed sequences of human Tyrosinase and have organized a non-redundant data set (table 1). The tyrosinases were retrieved in FASTA format and used for analysis.

Table 1
Human cyclooxygenase sequences retrieved from Swiss-Prot database.

Accession number	Sequence description	organism
P14679	Tyrosinase	Homo sapiens (Human)
P40126	L-dopachrome tautomerase	Homo sapiens (Human)
P17643	5,6-dihydroxyindole-2-carboxylic acid oxidase	Homo sapiens (Human)
075030	micropthalmia associated transcription factor	Homo sapiens (Human)
Q04671	P Protein	Homo sapiens (Human)
P21583	Kit ligand	Homo sapiens (Human)

2.2 Computational tools and servers

The number of cleaveges and the site of cleavage of the enzyme chymotrypsin and trypsin is calculated by the Ex-Pasy's peptide cutter tool for all the six sequences of tyrosinase are tabulated in table 2 and the amino acid composition (table 3) of tyrosinase sequences were computed using the tool CLC *free Workbench.*[22] Percentages of hydrophobic and hydrophilic residues were calculated from the primary structure analysis results and tabulated in table 4. The physico-chemical parameters, theoretical isoelectric point (pI), molecular weight, total number of positive and negative residues, extinction coefficient,[23] half-life,[24–27] instability index,[28] aliphatic index[29] and grand average hydrophathy[30] (GRAVY) were computed using the Expasy's ProtParam (http://us.expasy.org/tools/ protparam.html) prediction server and tabulated in table 5. The tools SOPMA[31] and Secondary Structural Content Prediction (SSCP method-I) server[32] were used for the secondary structure prediction. The SOSUI[33] server performed the identification of transmembrane regions (table 5). The predicted trans-membrane helices were plotted using Kite and Doolittle score (figure 1). Predicted trans-membrane helices were visualized and analyzed using helical wheel plots (figure 2) generated by the program Pepwheel[34] included in the EMBOSS 2.7 suite. Tyrosinases P14679, P40126, P17643, Q04671, 075030 and P21583 are predicted by CYS_REC.[35] CYS_REC identifies the positions of cysteines, total number of cysteines present and predicts the most probable SS bond pattern of pairs in the protein sequence.. The 3D structure of tyrosinase P14679 was generated by homology modeling using Esypred[36] server. The similar 3D structure (for the tyrosinase P14679 sequences) in the Protein Data bank (www.rscb.org) was identified by the BLASTP analysis (http://www.ncbi.nlm.nih.gov:80 /BLAST/) in table 7. The modeled 3D structures were evaluated using the online servers Rampage,[37] and ProQ[38] (Protein Quality server). The tool Rasmol (http://openrasmol.org/) and SwissPdbviewer [39](http://spdbv.vital_it.ch/) are used to visualize the modeled 3D structures and to identify the SS bonds.

Table 2

Number of Cleavages and Positions of cleavage site for the enzyme chymotrypsin and trypsin of human tyrosinase are calculated using Expasy's peptide-cutter.

Accession ID	Name of enzyme	No. of cleavages	Positions of cleavage site
P14697	Chymotrypsin	63	7 11 13 39 71 84 85 95 98 105 107 108 124 134 137 149 156 167 173 176 181 182 195 200 207 210 214 218 231 235 236 238 251 268 269 272 282 320 327 338 340 347 369 386 392 397 400 425 429 433 438 439 447 449 451 460 463 467 475 477 521 525
	Trypsin	42	22 28 33 43 52 77 87 104 115 116 120 121 133 142 160 196 221 217 224 239 243 278 298 211 309 306 308 311 334 341 402 422 434 443 465 473 501 503 504 505 511 518
P40126	Chymotrypsin	56	5 6 8 71 75 90 91 101 104 111 113 141 156 163 176 182 184 185 187 190 191 204 209 216 219 222 240 244 245 247 262 279 282 292 303 334 339 340 345 347 354 375 392 398 403 410 430 435 445 453 455 487 492 495 502 515
	Trypsin	46	16 27 38 43 58 65 78 83 88 89 93 96 110 120 121 127 138 149 150 151 194 205 221 229 233 251 275 278 308 314 318 323 326 333 348 356 408 409 428 496 497 499 500 503
P17643	Chymotrypsin	52	13 19 94 95 105 117 144 159 179 185 187 188 190 193 194 200 208 213 220 223 226 244 248 249 251 272 283 286 296 342 347 348 355 362 369 383 400 406 411 414 418 438 443 453 462 464 473 494 499 519 522
	Trypsin	44	5 23 28 37 55 62 64 84 87 93 97 118 125 130 131 138 141 146 152 153 164 165 197 198 225 230 233 255 269 287 312 313 326 356 368 374 416 417 436 471 502 504 505 528
O75030	Chymotrypsin	17	11 17 24 25 85 129 142 196 197 199 237 265 325 348 360 457 471
	Trypsin	52	22 28 33 56 60 65 73 74 79 89 118 128 136 50 193 198 204 217 289 290 304 308 310 312 313 321 324 330 332 340 347 350 355 362 363 366 370 372 377 379 380 386 391 400 420 423 476 480 509 513 514
Q04671	Chymotrypsin	67	61 68 71 94 116 120 127 134 138 177 184 186 194 204 215 264 274 277 292 322 342 347 382 392 401 406 407 409 415 423 439 449 474 505 508 513 531 532 537 554 593 604 632 635 637 638 642 652 660 670 679 684 685 689 703 730 744 770 774 802 804 806 809 810 827 837
	Trypsin	67	6 9 10 35 36 37 40 53 74 76 88 90 102 108 111 137 142 155 165 167 170 172 173 179 202 246 263 265 281 282 290 297 305 324 352 413 416 419 421 455 465 499 500 528 534 535 539 548 555 560 566 572 573 578 588 589 595 602 613 614 616 625 676 713 720 811
P21583	Chymotrypsin	23	7 13 19 51 57 69 88 98 127 135 140 141 144 151 154 183 215 224 230 232 236 237 270
	Trypsin	32	2 3 24 30 32 38 42 49 56 87 103 116 121 124

Table 3
Amino acid composition (in %) of human cyclooxygenase computed using CLC free Workbench.

Acid	ACCESION ID					
	P14679	P40126	P17643	O75030	Q04671	P21583
Ala	5.7	5.2	5.8	5.5	9.4	4.8
Cys	3.2	3.7	3.2	1.9	1.8	1.8
Asp	5.7	5.8	5.8	4.2	3.0	6.2
Glu	5.1	4.2	5.4	8.0	5.7	6.6
Phe	5.9	6.2	5.8	1.5	4.5	5.1
Gly	6.4	6.9	6.3	4.2	6.3	2.2
His	3.2	2.9	2.8	2.7	3.2	0.7
Ile	4.2	2.5	3.4	4.8	6.3	5.9
Lys	3.2	3.1	1.9	5.1	2.3	8.1
Leu	10.4	11.4	9.1	10.3	14.6	10.6
Met	2.8	1.9	1.9	3.8	2.6	2.6
Asn	5.1	5.4	5.8	5.9	2.5	5.9
Pro	6.2	6.9	7.3	7.2	4.3	5.5
Gln	4.3	4.2	4.1	7.6	3.2	2.6
Arg	5.1	6.6	6.9	5.3	6.1	4.0
Ser	9.6	6.0	7.3	9.5	7.6	11.4
Thr	3.6	6.0	6.1	6.5	4.5	4.8
Val	3.2	5.4	6.1	4.2	8.0	8.1
Trp	2.6	2.5	1.7	0.2	2.0	1.5
Tyr	4.3	3.3	3.5	1.7	1.9	1.8

Table 4
Hydrophilic and hydrophobic residues content.

Accession Number	Percentage of hydrophobic residues	Percentage of hydrophilic residues	Net hydrophobic residues content
P14679	49.2	50.6	low
P40126	47.5	52.6	very low
P17643	49.5	50.6	low
075030	56.6	43.6	Very high
Q04671	40	59.8	Very low
P21583	52.1	48.1	Very high

Table 5
Parameters computed using Expasy's protParam tool.

Accession Number	Sequence length	M. wt	pI	-R	+R	EC	II	AI	GRAVY
P14679	529	60393.2	5.71	57	44	112270	56.76	71.76	-0.356
P40126	519	59145.3	6.73	52	50	97955	43.86	74.95	-0.323
P17643	537	60724.3	5.62	60	47	78810	49.85	72.25	-0.377
O75030	526	58795.4	5.93	64	55	19535	63.82	76.22	-0.660
Q04671	838	92849.5	6.84	73	70	118215	47.04	114.06	-0.364
P21583	273	30898.5	5.86	35	33	29700	49.34	92.42	-0.191

M. wt., Molecular weight; pI, Isoelectric point; –R, Number of negative residues; +R, Number of positive residues; EC, Extinction coefficient at 280 nm; II, Instability index; AI, Aliphatic index; GRAVY, Grand Average Hydropathy.

Figure 1
Kyte and Doolittle mean hydrophobicity profile computed for the transmembrane regions of tyrosinases P14679, P40126, P17643, Q04671, 075030 and P21583 (primary helices).

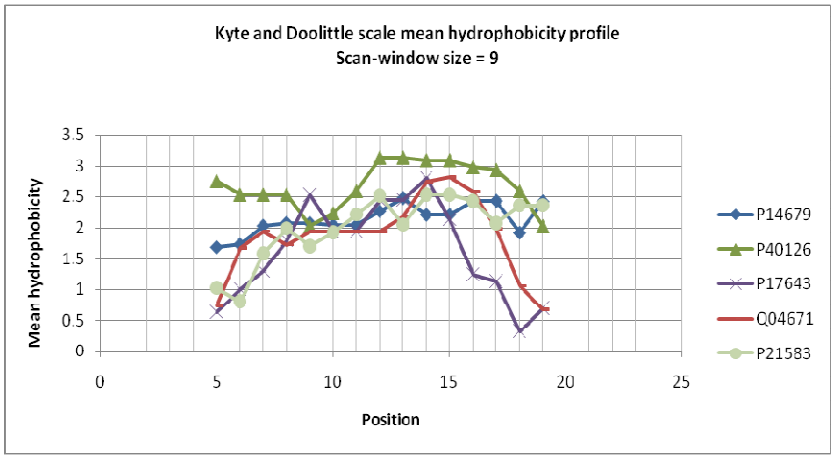

Table 6
Transmembrane regions identified by SOSUI server.

Accession number	Transmembrane region	Type	Length
P14679	MLLAVLYCLLWSFQTSAGHFPR	PRIMARY	22
	SWLLGAAMVGAVLTALLAGLVSL	PRIMARY	23
P40126	LLVVMGTLVALVGLFVLLAFLQY	PRIMARY	23
P17643	SAPKLLSLGCIFFPLLLFQQARA	PRIMARY	23
	EIIAIAVVGALLLVALIFGTASY	PRIMARY	23
Q04671	QWLKVMGLFAFVVLCSILFSLYP	PRIMARY	23
	SVETQVTIATAILAGVYALIIFE	PRIMARY	23
	RTLAAMLGSLAALAALAVIGDRP	PRIMARY	23
	DFETLALLFGMMILVAIFSETGF	PRIMARY	23
	WAMIIMLCLIAAVLSAFLDNVTT	PRIMARY	23
	MGLDFAGFTAHMFIGICLVLLV	SECONDARY	23
	DGILLAKCLTVLGFVIFMFFLNS	PRIMARY	23
	LDLGWIAILGAIWLLILADIHDF	PRIMARY	23
	WATLLFFAALFVLMEALAHLHLI	PRIMARY	23
	TALLIKMVPEEQRLIAAIVLVVW	SECONDARY	23
	MYALAFGACLGGNGTLIGASANV	SECONDARY	23
	RLGFPMMVVSCTVGMCYLLVAHV	PRIMARY	23
P21583	TWILTCIYLQLLLFNPLVKTEGI	SECONDARY	23
	LHWAAMALPALFSLIIGFAFGAL	PRIMARY	23

Table 7
PDB templates (first 2 hits with maximum % identity) using BLASTP search against the Protein Data Bank.

Accession number	PDB code	
P14679	3NM8_A	3NQ5_A

The three dimensional structure of tyrosinase P14679 modeled using the PDB template 3NM8_A is shown in figures 3 and 4. The six tyrosinase sequences with number of CYS and disulphide bond pattern predicted by CYS_REC are shown in table 8.

Table 8
No. of CYS and Disulfide (SS) bond pattern of pairs predicted, by CYS_REC (using primary structure)

Accession number	No. of CYS	CYS_REC
P14679	17	Cys24-Cys247 Cys36-Cys89 Cys46-Cys103 Cys55-Cys100 Cys91-Cys276 Cys112-Cys321 Cys244-Cys289
P40126	19	Cys12-Cys95 Cys15-Cys109 Cys29-Cys97 Cys40-Cys52 Cys61-Cys257 Cys106-Cys268 Cys118-Cys254
P17643	17	Cys41-Cys99 Cys42-Cys261 Cys56-Cys258 Cys65-Cys110 Cys101-Cys336 Cys113-Cys303 Cys122-Cys521
O75030	10	Cys3-Cys4
Q04671	15	Cys51-Cys457 Cys93-Cys410
P21583	5	Cys114-Cys163

3. RESULTS AND DISCUSSION

The results of primary structure analysis suggest that most of the tyrosinase are hydrophobic in nature due to the presence of high non -polar residues content (tables 3 and 4). The presence of high Cys residues in tyrosinases P14679, P40126, P17643, Q04671, 075030 and P21583 indicates the presence of disulphide bridges (SS bonds) in these tyrosinases. Moreover, the primary structure analysis suggests that the tyrosinase has high residues of acidic and basic amino acid, this might be involves in salt bridge formation. The average molecular weight of tyrosinase calculated is 60467.7 Da. Isoelectric point (pI) is the pH at which the surface of protein is covered with charge but net charge of the protein is zero. At pI proteins are stable and compact. All of the six human tyrosinases P14679, P40126, P17643, Q04671, 075030 and P21583 have (pI < 7) reveals that all of them are acidic in character. The computed isoelectric point (pI) will be useful for developing buffer systems for purification by isoelectric focusing method. Although Expasy's ProtParam computes the extinction coefficient for a range of (276, 278, 279, 280 and 282 nm) wavelength, 280 nm is favored because proteins absorb strongly there while other substances commonly in protein solutions do not. Extinction coefficient of tyrosinase at 280 nm is ranging from 19535 to 112270 M^{-1} cm^{-1} with respect to the concentration of Cys, Trp and Tyr. The high extinction coefficient of P14679 and Q04671 indicates presence of high concentration of Cys, Trp and Tyr. Similarly, the low extinction coefficient of 075030 indicates low concentration of Cys, Trp and Tyr. Rest of the tyrosinases have average extinction coefficient. The computed protein concentration and extinction coefficients help in the quantitative study of protein–protein and protein–ligand interactions in solution. The biocomputed half-life of most of the tyrosinases are 30 h in mammalian reticulocytes, invitro, greater than 20 h in yeast, in vivo and greater than 10h in *E.coli*, invivo. On the basis of instability index Expasy's ProtParam classifies all the tyrosinases as unstable (Instability index > 40).

The aliphatic index (AI) which is defined as the relative volume of a protein occupied by aliphatic side chains (A, V, I and L) is regarded as a positive factor for the increase of thermal stability of globular proteins. The lower thermal stability of the tyrosinases is indicative of a more flexible structure (table 5). The low aliphatic index of most of the tyrosinases infers that it may be thermolabile for a high range of temperature. Grand Average hydropathy (GRAVY) Index of tyrosinases are ranging from –0.660 to -0.191. The very low GRAVY index of tyrosinases infers that these tyrosinases could result in a better interaction with water. The secondary structure predicted with the help of programs SOPM and SOPMA (table 9) infers that the some of the tyrosinases have rich alanine content and mostly *α*-helices. Most of the tyrosinases have mixed secondary structure, i.e. *α*-helices, β-strands and coils. The very high coil structural content of tyrosinases is due to the rich content of more flexible glycine and hydrophobic proline amino acids. Proline has a special property of creating kinks in polypeptide chains and disrupting ordered secondary structure.

Table 9
Secondary structure calculation (in %) of human cyclooxygenase computed using SOPMA.

Accession number	Secondary Structure			
	Alpha Helix	Beta Sheet	Random Coil	Others
P14679	31.38	10.59	55.20	2.84
P40126	29.09	14.07	53.37	3.47
P17643	30.91	10.61	55.87	2.61
O75030	38.02	6.46	52.66	2.85
Q04671	49.16	16.95	27.92	5.97
P21583	50.55	7.33	39.56	2.56

The server SOSUI classifies the tyrosinases P14679, P40126, P17643, Q04671, and P21583 as membrane protein and 075030 tyrosinase as soluble protein. SOSUI server has identified transmembrane region in the tyrosinases P14679, P40126, P17643, Q04671, and P21583. The transmembrane regions and their length are tabulated in table 6. The transmembrane regions are rich in hydrophobic amino acids and it is also well documented by Kyte and Dolittle mean hydrophobicity profiles (figure 1) in which all the points are above the 0.0 line except P17643. The helix of P40126 is visualized using EMBOSS pep-wheel shown in figure 2.

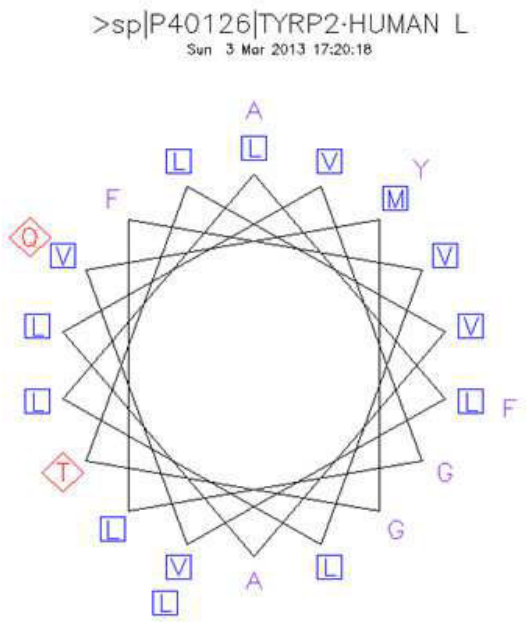

Figure 2

Helical wheel representation of predicted helix of P40126 tyrosinase. Hydrophobic residues (V, L, I) are represented as blue squares and violet letters (A, G, P, Y), polar residues (E, Q, S, T) as red diamonds.

The three dimensional structure of tyrosinase P14679 was modeled using PDB template (table 7) selected from the hits obtained through the BLASTP analysis and the modeled structures were evaluated. According to evaluation analysis, the Ramachandran plot and other parameters (table 10) were within the standard acceptable limits for the 3D structures modeled using the PDB template 3NM8_A for the (target) protein.

Table 10

Validation parameters computed for the built 3D structures of target P23219.

		Rampage	Procheck	ProQ	
Target	Template (PDB codes)	Percentage residues in favored region	Percentage of residues In favored region	LG score	maxsub
P14679	3NM8_A	89.5	83.4	3.06	0.32

Table 11

Criteria for a good (model) 3D structure.

Rampage	Procheck	ProQ		
Percentage of residues In favored region	Percentage of residues In favored region	LG score	maxsub	Quality of the model
98	90	>1.5	>0.1	Fairly good model
		>2.5	>0.5	Very good model
		>4.0	>0.8	extremely good model

A criterion for a good 3D structure is given in table 11. The modeled structure is visualized by the VEGA ZZ[40] and SPDBV tools and shown in fig.3 (a) and 3(b) as wireframe and protein backbone respectively. Helix and strand are also shown separately in the figure (5).the modeled structures are evaluated by Rampage, Procheck and ProQ software. The parameters are given in the table (9), which fulfills the criteria of very good model. Moreover, the Ramachandran plot after evaluation with Procheck suggests only 1.5% residues are in disallowed region, which is shown in the figure4.

Figure 3(a)

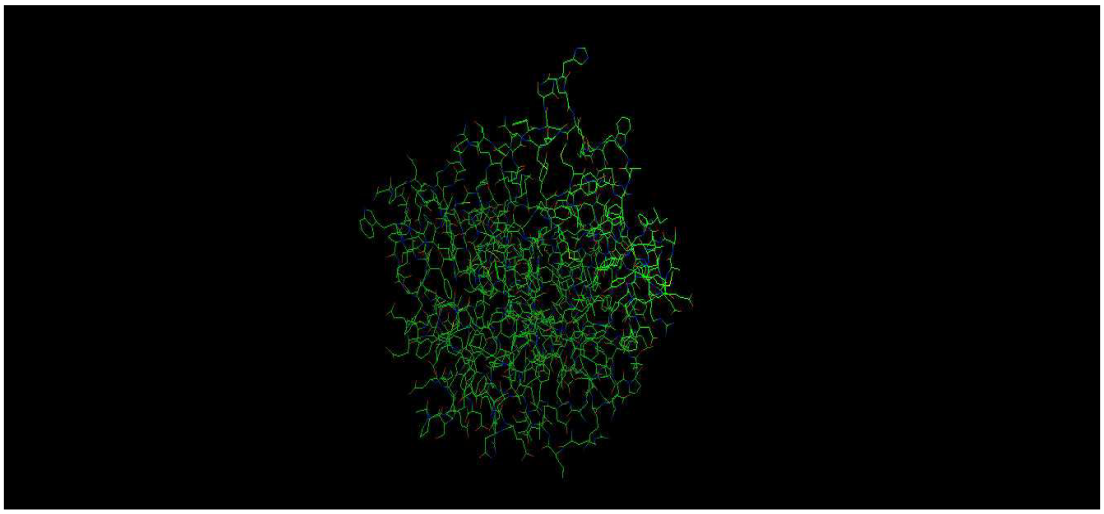

VEGA ZZ (wireframe diagram) representation of the homology modeled 3D structure of tyrosinase P14679 (using PDB template 3NM8_A).

Figure 3(b)

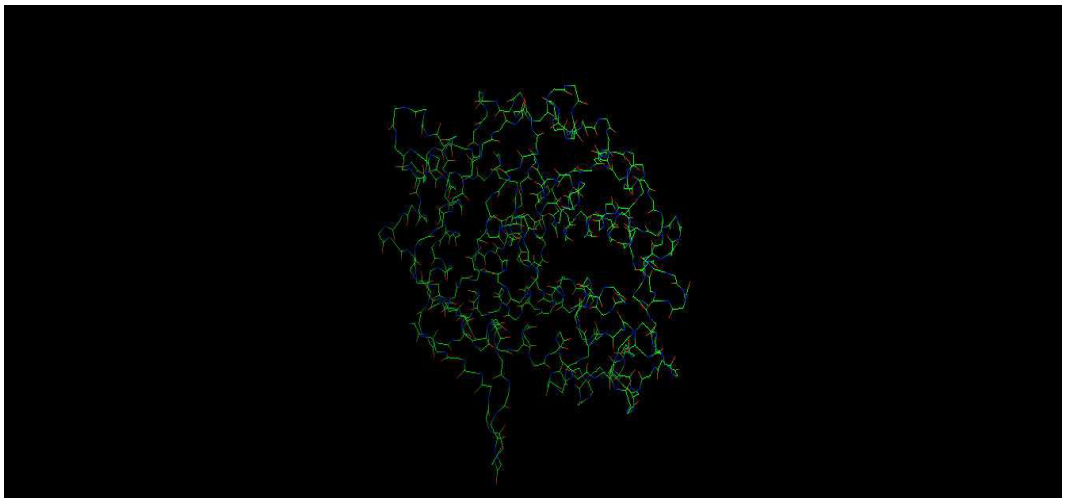

VEGA ZZ (protein backbone) representation of the homology modeled 3D structure of tyrosinase P14679 (using PDB template 3NM8_A).

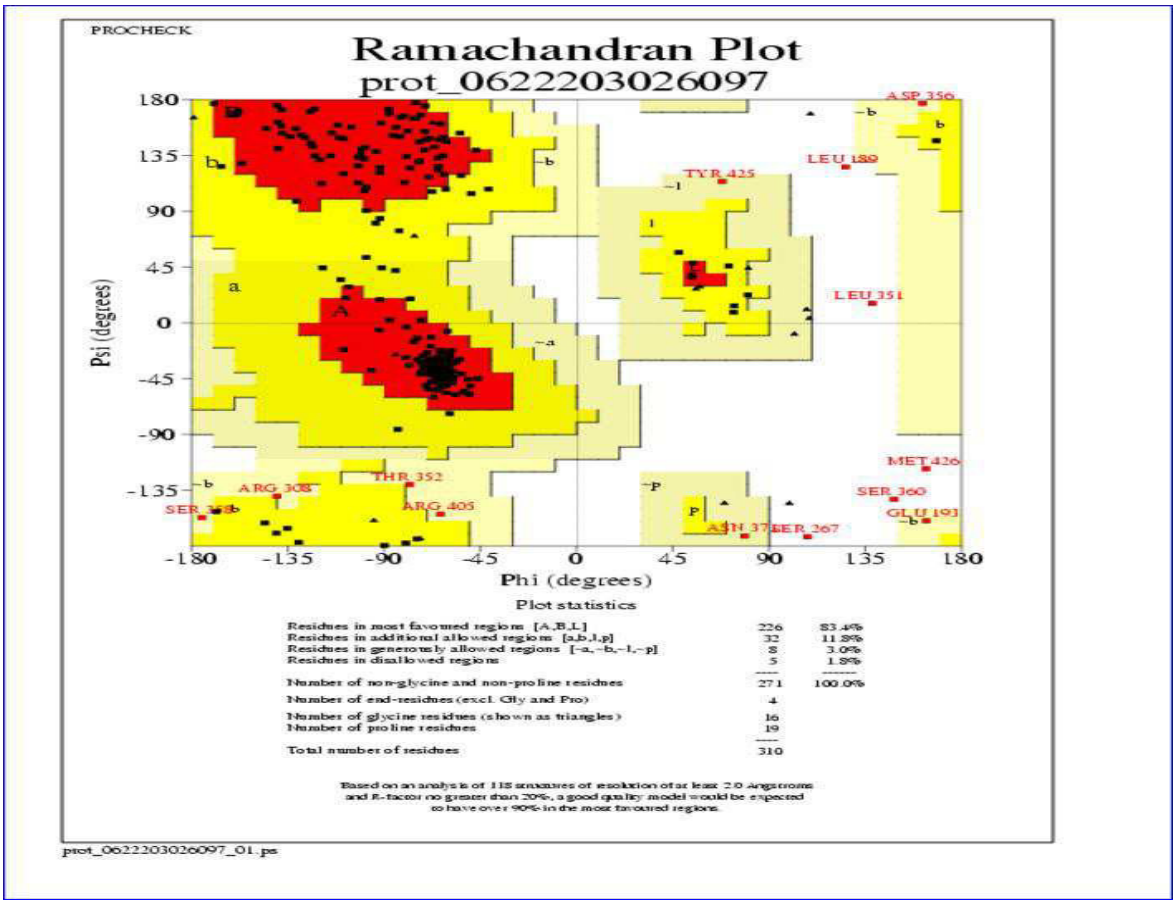

Figure 4
Ramachandran plot after evaluation by PROCHECK.

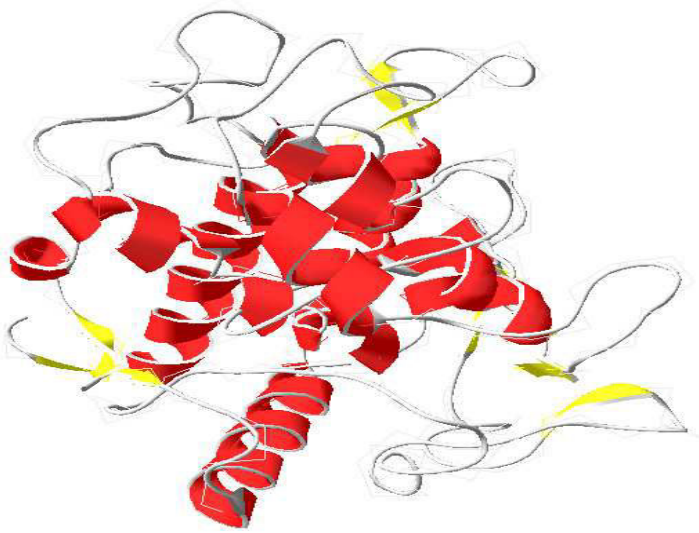

Figure 5
homology modeled 3D (SPDBV) structure of tyrosinase P14679 (using PDB template 3NM8_A) showing secondary structure.

4. CONCLUSION

Six human tyrosinase have been chosen mainly to study their physico-chemical properties, primary and secondary structures by using computational tools and servers. Primary structure analysis reveals that most of the tyrosinase under study are hydrophobic in nature and all of them contain disulphide linkages. Physico-chemical characterization studies give a good idea about the properties such as pI, EC, AI, GRAVY and Instability Index that are essential and vital in providing data about the proteins and their properties. Secondary structure analysis predicts that some of them contain α-helices and remaining of them contains mixed structure.

5. ACKNOWLEDGEMENT

Authors are grateful to the Department of Biotechnology (DBT), MST, Govt. of India for the computational laboratory facility.

6. REFERENCES

1. Sivakumar K 2005 *Adv. BioTech.* IV 27
2. Sivakumar K, Balaji S and Gangaradhakrishnan *Bio-Chemistry: An Indian Journal* (in press)
3. Sivakumar K 2006 *Adv. BioTech.* IV 18
4. King-Hwa Ling, Shu-San Loo, Rozita Rosli, Mariana Nor Shamsudin, Rahmah Mohamed and Kiew-Lian Wan 2007 *Silico Biol.* 7 0011
5. Chitta Suresh Kumar, Anuradha C M, Venkata Rao K and Venkateswara Swamy K 2005 *Int. J. Genomics Proteomics* 2 1
6. Yuri F, Bogdanov, Sergei Y, Dadashev and Tatiana M Grishaeva 2003 *Silico Biol.* 3 0015
7. Courtney E Garry and Robert F Garry 2004 *Theor. Biol. Med. Model.* 1 10
8. Rachel E Bell and Nir Ben-Tal 2003 *Comp. Funct. Genom.* 4 420
9. Gao L, Fang JS, Bai XY, Zhou D, Wang YT, Liu AL, Du GH.Chem Biol Drug Des. 2013 Mar 5. doi: 10.1111/cbdd.12127
10. Liu J, Chen C, Wu F, Zhao L.Chem Biol Drug Des. 2013 Mar 5. doi: 10.1111/cbdd.12126
11. Sung YM, Gayam SR, Wu SP.Appl Biochem Biotechnol. 2013 Mar 2
12. Hildén K, Mäkelä MR, Lankinen P, Lundell T.Fungal Genet Biol. 2013 Feb 20
13. Chon SU.Curr Pharm Des. 2013 Feb 19
14. Silveira JP, Seito LN, Eberlin S, Dieamant GC, Nogueira C, Pereda MC, Di Stasi LC.BMC Complement Altern Med. 2013 Feb 27;13(1):49.
15. Ren Q, Henes B, Fairhead M, Thöny-Meyer L.BMC Biotechnol. 2013 Feb 27;13(1):18.
16. Lin L, Lei F, Sun DW, Dong Y, Yang B, Zhao M.Food Chem. 2012 Oct 15;134(4):2021-9.
17. Kamagaju L, Morandini R, Bizuru E, Nyetera P, Nduwayezu JB, Stevigny C, Ghanem G, Duez P.J Ethnopharmacol. 2013 Feb 22.
18. Mu Y, Li L, Hu SQ.Spectrochim Acta A Mol Biomol Spectrosc. 2013 Feb 1;107C:235-240.
19. JENNIFER, C. , STEPHIE, C.M., ABHISHRI, S.B. AND SHALINI B. U* Int J Pharm Bio Sci 2012 Oct; 3(4): (B) 332 – 347
20. K P BALAKRISHNAN, NITHYA NARAYANASWAMY AND ARUN DURAISAMY Int J Pharm Bio Sci vol 2/issue 1/ jan-mar 2011
21. Lin YF, Hu YH, Lin HT, Liu X, Chen YH, Zhang S, Chen QX.J Agric Food Chem. 2013 Mar 4.
22. CLC bio., 2006. CLC free Workbench. http://www. clcbio.com/index.php?id=28, (27/10/2006)

23. Gill S C and Von Hippel P H 1989 *Anal. Biochem* 182 319
24. Bachmair A, Finley D and Varshavsky A 1986 *Sci ence* 234 179
25. Gonda D K, Bachmair A, Wunning I, Tobias J W, Lane W S and Varshavsky A 1989 *J. Biol. Chem.* 264 16700
26. Tobias J W, Shrader T E, Rocap G and Varshavsky A 1991 *Science* 254 1374
27. Ciechanover A and Schwartz A L 1989 *Trends Bio chem. Sci.* 14 483
28. Guruprasad K, Reddy B V B and Pandit M W 1990 *Prot. Eng.* 4 155
29. Ikai A 1980 *J. Biochem.* 88 1895
30. Kyte J and Doolittle R F 1982 *J. Mol. Biol.* 157 105
31. Combet C, Blanchet C, Geourjon C and Deléage G 2000 *TIBS* 25 291, 147
32. Eisenhaber F, Imperiale F, Argos P and Froemmel C 1996 *Proteins Struct. Funct. Design* 25 157
33. Takatsugu Hirokawa, Seah Boon-Chieng and Shigeki Mitaku 1998 *Bioinform. Appl. Note* 14 378
34. Ramachandran G N and Sasiskharan V 1968 *Adv. Prot. Chem.* 23 283
35. CYS_REC.http://sun1.softberry.com/berry.phtml?topic=cys_rec&group=help&subgroup=propt. (27/10/2006)
36. Lambert C, Leonard N, De Bolle X and Depiereux E 2002 *Bioinformatics* 18 1250
37. Lovell. S C, Davis I W, Arendall III W B, de Bakker P I W, Word J M, Prisant M G, Richardson J S and Richardson D C 2002 *Proteins: Structure, Function & Genetics* 50 437
38. Cristobal S, Zemla A, Fischer D, Rychlewski L and Elofsson A 2001 *BMC Bioinformatics* 2 5
39. F Kiefer, K Arnold, M kunzli, L Bordoli, T Schwede, , Nucleic Acids Research. 37, 2009 D387-D92
40. Pedretti, L.Villa, g.Vistoli J.Mol. Graph., Vol.21, 47-49 (2002)